Bogoliubov angle and visualization of particle-hole mixture in superconductors

K. Fujita,[1] Ilya Grigorenko,[2] J. Lee,[1] W. Wang,[1] Jian Xin Zhu,[3] J. C. Davis,[1,4] H. Eisaki,[5] S. Uchida,[6] and Alexander V. Balatsky[7]

[1]*LASSP, Department of Physics, Cornell University, Ithaca, New York 14853, USA*

[2]*Theoretical Division T-11, Center for Nonlinear Studies, Center for Integrated Nanotechnologies, Los Alamos National Laboratory, Los Alamos, New Mexico 87545, USA*

[3]*Theoretical Division, Los Alamos National Laboratory, Los Alamos, New Mexico 87545, USA*

[4]*CMPMS Department, Brookhaven National Laboratory, Upton, New York 11973, USA*

[5]*Nanoelectronics Research Institute, AIST, Ibaraki 305-8568, Japan*

[6]*Department of Physics, The University of Tokyo, Tokyo 113-0033, Japan*

[7]*Theoretical Division and Center for Integrated Nanotechnologies, Los Alamos National Laboratory, Los Alamos, New Mexico 87545, USA*

(Received 4 September 2007; revised manuscript received 17 June 2008; published 13 August 2008)

Superconducting excitations—Bogoliubov quasiparticles—are the quantum-mechanical mixture of negatively charged electron $(-e)$ and positively charged hole $(+e)$. Depending on the applied voltage bias in scanning tunneling microscope (STM), one can sample the particle and hole contents of such a superconducting excitation. Recent STM experiments offer unique insight into the inner workings of the superconducting state of superconductors. We propose an observable quantity for STM studies that is a manifestation of the particle-hole dualism of the quasiparticles. We call it a *Bogoliubov angle*. This angle measures the relative weight of particle and hole amplitudes in the superconducting (Bogoliubov) quasiparticle. We argue that this quantity can be measured locally by comparing the ratios of tunneling currents at positive and negative biases. This Bogoliubov angle allows one to measure directly the energy and position dependent particle-hole admixtures and therefore visualize robustness of superconducting state locally. It may also allow one to measure the particle-hole admixture of excitations in normal state above critical temperature and thus may be used to measure superconducting correlations in pseudogap state.

DOI: 10.1103/PhysRevB.78.054510 PACS number(s): 74.20.−z, 71.27.+a, 68.37.Ef

I. INTRODUCTION

The dual particle wave character of microscopic objects is one of the most striking phenomena in nature. This dualism is ubiquitous in the microworld. Most notably, the two slit experiments of Stern and Gerlach revealed the interference and, hence, the wave nature of electrons. In the condensed-matter systems, such an explicit visualization of the wave nature of the constituent electrons was missing until just recently. The breakthrough came when the researchers from the IBM laboratories realized that the best way to elucidate the electrons *inside* a material is to place an impurity in an otherwise perfect crystal structure. By building corrals of the impurities on the clean surface and by observing the generated patterns through the scanning tunneling microscope (STM), the experimenters were able to demonstrate the laws of the wave optics using the conduction-electron waves.[1–3]

The analog of the conduction electrons in the superconductors are the quasiparticles. Unlike electrons, the superconducting quasiparticles do not carry definite charge. The same quantum-mechanical dualism is at play when one considers the Bogoliubov quasiparticles in superconducting state: the quasiparticle is a coherent combination of an electron and its absence (hole):[4] its annihilation operator is a linear combination of particle and hole operators with the amplitudes $u_{\mathbf{k}}, v_{\mathbf{k}}$: $\gamma_{\mathbf{k},\uparrow}=u_{\mathbf{k}}c_{\mathbf{k},\uparrow}+v_{\mathbf{k}}^{*}c_{-\mathbf{k},\downarrow}^{\dagger}$. Particle-hole dualism of quasiparticles is responsible for a variety of profound phenomena in superconducting state such as Andreev reflection, the particle-hole conversion process that is only possible in superconductor.

In this paper we propose a technique to reveal this coherent particle-hole mixture locally. In order to discuss the particle-hole mixture we introduce a quantity that parametrizes the mixture in terms of an angle, and we call this angle a Bogoliubov angle (BA), see Fig. 1. We argue that STM measurements allow us to visualize the Bogoliubov angle maps and thus to reveal particle-hole dualism. Bogoliubov angle maps as a function of position and energy offer a tool to investigate strength of superconducting state locally.

To illustrate the point about BA, we can look at the uniform BCS case first.[4] In the normal state and in the presence of translational invariance we use plane waves as a basis, and therefore, amplitudes that are used in Bogoliubov transformation become functions of momentum $u_{\mathbf{k}}, v_{\mathbf{k}}$. These amplitudes are step functions of momentum and there is no mixing

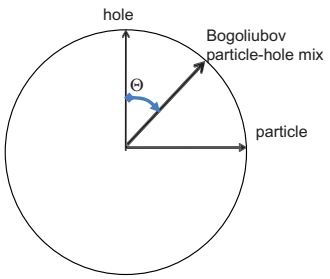

FIG. 1. (Color online) Circle parametrizing Bogoliubov admixture angle is shown. For $\Theta=0,90$ deg the mixture reduces to purely hole-like and particle-like states. At arbitrary angle one deals with true Bogoliubov quasiparticles.

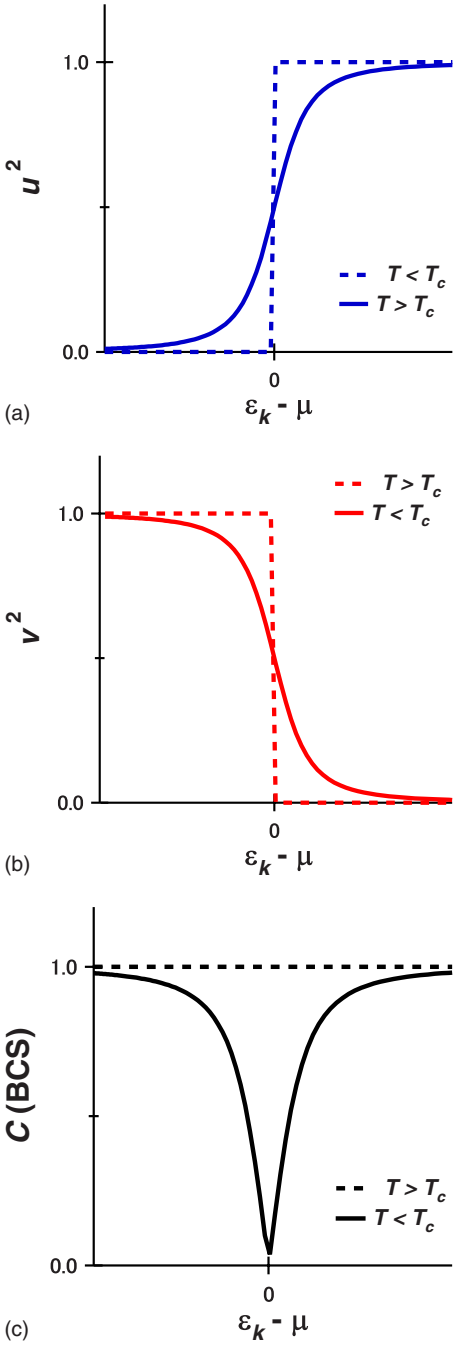

FIG. 2. (Color online) BCS factors $|u(\mathbf{k})|^2$ (blue) and $|v(\mathbf{k})|^2$ (red) are shown as functions of energy. The function $C(\mathbf{k})=|u^2(\mathbf{k})-v^2(\mathbf{k})|=|\cos 2\Theta(\mathbf{k})|$ (black) shows substantial departures from unity only in the energy range on the scale of the gap Δ near the Fermi energy where there are substantial pairing correlations.

between the particle and hole components of Bogoliubov quasiparticle. Once superconductivity sets in, the mixing between these components develops, Fig. 1. Using Bogoliubov amplitudes, we introduce BA as

$$\Theta_k = \arctan\left\{\left[\frac{|u(\mathbf{k})|^2}{|v(\mathbf{k})|^2}\right]^{1/2}\right\}, \tag{1}$$

with the conventional factors, see Fig. 2. Here we do not differentiate between s-wave and d-wave superconducting states. The only difference between these cases will come from angular dependence of $|u(\mathbf{k})|^2$ and $|v(\mathbf{k})|^2$.

Next we consider an inhomogeneous superconductor when translational symmetry is broken by disorder.[5] We will use a mean-field approach and mostly focus on $T=0$. We start from a rather general description of nonuniform superconductor, which allows three different kinds of random impurities: scalar impurity, magnetic impurity, and local superconducting gap variations. In the simplified model, the conduction electrons occupy lattice sites, $\mathbf{r}_i$, and can hop to the neighboring sites, $\mathbf{r}_j$, with hopping matrix element t_{ij}.

$$\begin{aligned} H_0 = & \sum_{\langle \mathbf{r}_i,\mathbf{r}_j\rangle,\sigma} t_{ij} c^\dagger_{\mathbf{r}_i,\sigma} c_{\mathbf{r}_j,\sigma} + \Delta(\mathbf{r}_i,\mathbf{r}_j) c^\dagger_{\mathbf{r}_i,\sigma} c^\dagger_{\mathbf{r}_i,\sigma} \\ & + [V^s_{\mathrm{imp}}(\mathbf{r}_i) - \mu] n(\mathbf{r}_i) + V^M_{\mathrm{imp}} c^\dagger_{\mathbf{r}_i,\sigma} \sigma^z c^\dagger_{\mathbf{r}_i,\sigma} S_z \\ & + \delta\Delta(\mathbf{r}_i,\mathbf{r}_j) c^\dagger_{\mathbf{r}_i,\sigma} c^\dagger_{\mathbf{r}_j,\sigma}, \end{aligned} \tag{2}$$

were a quantum-mechanical operator $c^\dagger_{\mathbf{r}_i,\sigma}$ creates an electron on-site i, the operator $c_{\mathbf{r}_j,\sigma}$ eliminates an electron from the site j, and $n(\mathbf{r}_i)=c^\dagger_{\mathbf{r}_i,\uparrow}c_{\mathbf{r}_i,\uparrow}+c^\dagger_{\mathbf{r}_i,\downarrow}c_{\mathbf{r}_i,\downarrow}$ represents the electron-density on-site i. The electron spin, σ, can point up or down. Here σ^z is a Pauli matrix and S_z is a classical spin. The impurities may be modeled independently from each other and are given by the correspondent quantities: V^s_{imp} is a local scalar potential. This term is the potential of impurity that couples to the total electronic density on-site i. V^M_{imp} is a strength of the coupling of local magnetic impurity S_z with the electron spin and $\delta\Delta(\mathbf{r}_i,\mathbf{r}_j)$ is a superconducting impurity, which modulates the superconducting gap function. To model the high-temperature superconductors, we utilize the highly anisotropic structure of the cuprates and focus on a single layer of the material.

Given that the pairing of electrons occurs in the spin singlet state, the superconducting order-parameter amplitude can be expressed in the form,

$$F(\mathbf{r}_i,\mathbf{r}_j) = \sum_{\sigma,\mu} (i\sigma^y)_{\sigma,\mu} \langle c_{\mathbf{r}_i,\sigma} c_{\mathbf{r}_j,\sigma}\rangle. \tag{3}$$

The relation between the order parameter and the gap function is given by the self-consistency equation,

$$\Delta(\mathbf{r}_i,\mathbf{r}_j) = \eta(\mathbf{r}_{ij}) F(\mathbf{r}_i,\mathbf{r}_j), \tag{4}$$

where $\mathbf{r}_{ij}=(\mathbf{r}_i-\mathbf{r}_j)/2$ is the interparticle distance and η is the relative strength of the two-particle interaction.

Since Eq. (2) is quadratic in $c_{\mathbf{r}_i,\sigma}$, one can use a linear canonical transformation to diagonalize. Bogoliubov showed that fermionic operators are described by the unitary transformation from particle and hole operators to quasiparticles with the quasiparticle amplitudes $u_n(\mathbf{r}_i)$ and $v_n(\mathbf{r}_i)$:

$$c_{\mathbf{r}_i,\downarrow} = \sum_n [u_n(\mathbf{r}_i)\gamma_{n,\downarrow} + v_n^*(\mathbf{r}_i)\gamma_{n,\uparrow}^\dagger],$$

$$c_{\mathbf{r}_i,\uparrow} = \sum_n [u_n(\mathbf{r}_i)\gamma_{n,\uparrow} - v_n^*(\mathbf{r}_i)\gamma_{n,\downarrow}^\dagger]. \quad (5)$$

With this unitary transformation, one obtains a diagonal effective Hamiltonian: $H_{\text{eff}}=H_0+\Sigma_{n,\sigma}E_n\gamma_{n,\sigma}^\dagger\gamma_{n,\sigma}$. Here n refers to the eigenvalue index for the excitations above the ground state. Each eigenstate n is doubly degenerate (with no magnetic impurities) where for each state n there is a time-reversal partner, which we labeled n^*. Pairing involves paired states with n and n^*. Operators γ_n describe natural excitations in the superconducting state. Self-consistency condition implies that $\Delta(\mathbf{r}_i,\mathbf{r}_j)=\eta(\mathbf{r}_{ij})\Sigma_n v_n^*(\mathbf{r}_i)u_n(\mathbf{r}_j)$.

In continuum superconductors the amplitudes $u_n(\mathbf{r}),v_n(\mathbf{r})$ obey the constraints $\int d\mathbf{r}[u_m^*(\mathbf{r})u_n(\mathbf{r})+v_m^*(\mathbf{r})v_n(\mathbf{r})]=\delta_{nm}$ (normalization) and $\Sigma_n[u_n^*(\mathbf{r})u_n(\mathbf{r}')+v_n^*(\mathbf{r}')v_n(\mathbf{r})]=\delta(\mathbf{r}-\mathbf{r}')$ (completeness) for any $\mathbf{r}$ and $\mathbf{r}'$. The discrete analogs of the normalization and completeness relations for the amplitudes $u_n(\mathbf{r}_i),v_n(\mathbf{r}_i)$, with $\mathbf{r}_i$ and $\mathbf{r}_j$ being the sites in our lattice, are: $\int d\mathbf{r}_i[u_m^*(\mathbf{r}_i)u_n(\mathbf{r}_i)+v_m^*(\mathbf{r}_i)v_n(\mathbf{r}_i)]=\delta_{nm}$, and $\Sigma_n[u_n^*(\mathbf{r}_i)u_n(\mathbf{r}_j)+v_n^*(\mathbf{r}_j)v_n(\mathbf{r}_i)]=0$ where $(i\neq j)$, $\Sigma_n\,|u_n(\mathbf{r}_i)|^2+|v_n(\mathbf{r}_i)|^2]=1$, and $(i=j)$. The values $|u_n(\mathbf{r}_i)|^2$ and $|v_n(\mathbf{r}_i)|^2$ will enter into observable, local density of states (LDOS) in local tunneling experiments, see below.

Going to the problem at hand we want to focus on a similar language about amplitudes as a function of position. We define mixing strength as a position dependent angle,

$$\Theta_n(\mathbf{r}_i) = \arctan\left\{\left[\frac{|u_n(\mathbf{r}_i)|^2}{|v_n(\mathbf{r}_i)|^2}\right]^{1/2}\right\}, \quad (6)$$

which is a central quantity we are interested in. We define this quantity as a Bogoliubov angle. The high-resolution STM allows us to study the spatial dependence of the BA for the states whose energy can be selected by tuning STM bias.

Note, we intentionally do not simplify the expression in Eq. (6) for the reasons that will be clear in the next section. It represents a local mixture between particle and hole excitations for an eigenstate n at a given site i. For example, for $\Theta_n(\mathbf{r}_i)=0$ the Bogoliubov excitation will be a hole. In the opposite case of $\Theta_n(\mathbf{r}_i)=90$ deg quasiparticle is essentially an electron. The angle that corresponds to the strongest admixture between particle and hole is $\Theta_n(\mathbf{r}_i)=90$ deg. Obviously, in case of an inhomogeneous state the BA is a function of a position where it is measured and also is a function of energy E. We suggest a way to visualize the BA maps that allows us to develop a more detailed understanding of the superconducting state.

Previously the alternation of amplitudes u,v as functions of position near impurities has been discussed in Refs. 6–9. Here we expand this discussion by introducing local BA. We also will focus more on the spontaneous inhomogeneity when we use the STM data and not the impurity states that were the focus of previous studies.

The ideas presented here are quite general and are applicable to a variety of superconductors, including conventional superconductors. Imaging of BA can be performed in any inhomogeneous state. One can investigate BA in a variety of states, including vortex and normal states with superconducting correlations, e.g., so-called pseudogap (PG) state.[10,11] To illustrate this approach, we will use the local STM data obtained on high-T_c superconductor, namely on $Bi_2Sr_2CaCu_2O_{8+\delta}$ material.

The plan of the paper is as follows: In Sec. II we present a general theoretical background and define BA from the local tunneling conductance measurements $dI/dV(\mathbf{r},V)$ at different bias values V. In Sec. III we briefly discuss imaging of BA in normal and pseudogap state. In Sec. IV we discuss BA as seen in the STM data. In Sec. V we present numerical simulations of BA in superconductor with broken translational invariance. And in Sec. VI we conclude with the discussion of the obtained results.

II. THEORETIC DISCUSSION

We now turn to inhomogeneous problem where we can no longer use translational invariance and plane waves as a basis. Real-space description[5] used here is necessary in case we consider the effects of disorder in single-particle potential. Either kind of disorder breaks translational symmetry, and the real-space representation is more natural in this case. The self-consistently defined gap amplitude,

$$\Delta(\mathbf{r}_i,\mathbf{r}_j) = V_{\text{int}}\sum_n u_n(\mathbf{r}_i)v_n^*(\mathbf{r}_j)[1-2f(E_n)], \quad (7)$$

with $V_{\text{int}}=\eta(\mathbf{r}_i,\mathbf{r}_j)$ being an interaction on nearest sites and $f(E_n)$ being the Fermi distribution function for a given quasiparticle excitation spectrum E_n. Here E_n are defined to be positive only, as E_n represents the excitation energy for quasiparticles *above* the ground state. We assume that pairing interaction couples only nearest neighbors on the lattice $\mathbf{r}_j,\mathbf{r}_i$.

For a next step in our discussion it is necessary to introduce a tunneling conductance as measured by local STM tunneling. Let us introduce the tunneling conductance on positive and negative biases $E=\pm e|V|$ as

$$dI/dV_+(\mathbf{r}_i,E) = -F(z,|eV|)\sum_{n,s}|u_{n,s}|^2(\mathbf{r}_i)f'(E-E_n),$$

$$dI/dV_-(\mathbf{r}_i,E) = -F(z,-|eV|)\sum_{n,s}|v_{n,s}|^2(\mathbf{r}_i)f'(E+E_n), \quad (8)$$

where $F(z,\pm|eV|)$ is a function that measures the matrix elements for tunneling as a function of voltage bias and tip distance z. Hereafter we assume that it is a smooth function of energy and at small energies $E\sim 10-100$ meV it is a constant, thus we will assume that tunneling matrix element effect will only provide an overall coefficient in the LDOS. $f(E)$ is the Fermi distribution function. At very low temperatures $f'(E)$ becomes nearly $-\delta(E)$ function, a fact that we will use often. We can simplify the formulas if we introduce the density of states (DOS) for quasiparticles: $\rho(E)=\Sigma_{n,s}\delta(E-E_n)$. Here we stress that thus defined $\rho(E)$ is a density of states of quasiparticles, all of them being excitations above the ground state with $E>0$ and all of them hav-

ing a weight unity. As defined this quasiparticle DOS is not identical to the DOS of real electron and hole excitations. For simplicity we will assume particle-hole symmetry in the normal state.

Then, for a given eigenspectrum and eigenfunctions $u_n(\mathbf{r}_i), v_n(\mathbf{r}_i)$ we can rewrite Eq. (8) as

$$dI/dV_+(\mathbf{r}_i,|eV|) = -\int dE\rho(E)|u_{E,s}|^2(\mathbf{r}_i)f'(|eV|-E),$$

$$E \geq 0,$$

$$dI/dV_-(\mathbf{r}_i,|eV|) = -\int dE\rho(E)|v_{E,s}|^2(\mathbf{r}_i)f'(|eV|+E),$$

$$E \leq 0. \tag{9}$$

Here we used the assumption that dI/dV at a given tunneling point is proportional to the LDOS at this point with the tunneling matrix elements $F(z, \pm e|V|)$ being simply constants. LDOS for superconductor is defined $(T=0)$ as

$$N(\mathbf{r}_i,E) = -1/\pi\ \mathrm{Im}(\mathbf{r}_i,E) = \sum_n |u_n(\mathbf{r}_i)|^2\delta(E-E_n), \quad E>0,$$

$$= \sum_n |v_n(\mathbf{r}_i)|^2\delta(E+E_n), \quad E<0. \tag{10}$$

And we used the Nambu spinor notations to indicate that we are looking at particle Green's function, labeled as G_{11}.[4] Using these equations and quasiparticle density of states $\rho(E)$, we obtain Eq. (9).

Hence the ratio of dI/dV—taken at the same $|E|$—that we label as $Z(\mathbf{r}_i,|eV|)$, will be

$$Z(\mathbf{r}_i,|eV|=E) = \frac{dI/dV_+(\mathbf{r}_i,|eV|)}{dI/dV_-(\mathbf{r}_i,|eV|)} = \frac{|u_{E,s}|^2(\mathbf{r}_i)}{|v_{E,s}|^2(\mathbf{r}_i)} = \tan 2\Theta(\mathbf{r}_i,E), \tag{11}$$

where the last step is taken assuming that there are few—often one state—that contributes to the summation in Eq. (8), an energy $E=|eV|$. Then Eq. (11) can be inverted as

$$\Theta(\mathbf{r}_i,E) = \arctan\left\{\left[\frac{dI/dV_+(\mathbf{r}_i,|eV|)}{dI/dV_-(\mathbf{r}_i,|eV|)}\right]^{1/2}\right\}. \tag{12}$$

This result along with Eq. (6) is the main result of this section. It allows a direct determination of Bogoliubov angle $\Theta(\mathbf{r}_i,E)$ from the experimentally measured tunneling conductances at positive and negative biases.

BA as a measure of particle-hole admixture appears naturally in the Anderson mapping[12] of BCS model on the effective spin model. We briefly recall the mapping in Appendix A.

To visualize the local quasiparticle states, we employ the STM technique. Crucial aspect of the electron tunneling into the superconducting state that makes it qualitatively different from the tunneling in conventional metals is that the STM tip contains only the regular electrons that carry a unit of charge $(-e)$. We can inject either electrons or holes in superconductor. On the other hand, as pointed out earlier starting with Bogoliubov, quasiparticles that live inside the superconductor do not possess a well defined charge. Upon entering the superconductor, an electron/hole that arrived from the normal STM tip must undergo a transformation into the Bogoliubov quasiparticles native to the superconductor.[4] Hence electrons that are injected or extracted form superconductor would need to be "assembled" from Bogoliubov excitations. At any site and at specific bias this conversion into particles and holes will depend on relative weights $u_n(\mathbf{r}_i), v_n(\mathbf{r}_i)$. Hence the intensity of a tunneling signal will depend on these amplitudes.

Qualitatively, the spatial distribution of tunneling intensity can be understood as follows: Respective amplitudes of particle and hole parts of the Bogoliubov quasiparticle, are $u_n(\mathbf{r}_i)$ and $v_n(\mathbf{r}_i)$ for site i and for particular eigenstate n. Consider now a site where, say, $u_n(\mathbf{r}_i)$ is large and close to one. It follows from the completeness relation $\Sigma_n\ |u_n(\mathbf{r}_i)|^2 + |v_n(\mathbf{r}_i)|^2] = 1$ that for the same site the $v_n(\mathbf{r}_i)$ would have to be small since the completeness condition is almost fulfilled by $|u_n(\mathbf{r}_i)|^2$ term alone. Similarly, for the sites where $v_n(\mathbf{r}_i)$ has large magnitude, $u_n(\mathbf{r}_i)$ would have to be small. Recall now that large $u_n(\mathbf{r}_i)$ component would mean that quasiparticle has a large electron component on this site. Hence the electron will have large probability to tunnel into superconductor on this site and the tunneling intensity for electrons (positive bias) will be large. Conversely, for those sites the hole amplitude is small $|v(\mathbf{r}_i)| \ll |u(\mathbf{r}_i)|$ and the hole intensity (negative bias) will also be small. Similarly, for sites with large hole amplitudes $|v(\mathbf{r}_i)| \gg |u(\mathbf{r}_i)|$ the electron amplitude will be suppressed and this site will be bright on the hole bias. We observe alternation of the form,

$$|v_n(\mathbf{r}_i)|^2 \simeq 1, \quad |u_n(\mathbf{r}_i)|^2 \ll 1,$$

$$|v_n(\mathbf{r}_i)|^2 \ll 1, \quad |u_n(\mathbf{r}_i)|^2 \simeq 1. \tag{13}$$

Therefore if there is a particular pattern for the large particle amplitude (sampled on positive bias) on certain sites i, the complimentary pattern of bright sites for hole tunneling (on negative bias) will develop as a consequence of the inherent particle-hole mixture in superconductor. This "antiphase" behavior is a clear indication of the "natural quasiparticles" having both particle and hole characters. It is the main effect that can be visualized by considering $\Theta(\mathbf{r}_i,E)$ maps. Antiphase shift in positive and negative bias intensities is ubiquitously seen in tunneling spectra. The antiphase behavior of the components $|u_E(\mathbf{r}_i)|^2$, $|v_E(\mathbf{r}_i)|^2$ is explained here as a case of BA changing from particle to holelike configuration on alternating sites. We see that this is the case in our numerical simulations (see numerical simulations below) without any need to assume that only one state dominates the sum over states in Eq. (9). So the phenomenon is more general. We find it easiest to explain assuming only one term dominating. However, given numerical results it holds for broader cases.

We discuss it in more detail below when we turn to $\Theta(\mathbf{r}_i,E)$ maps.

A. Particle-hole asymmetry of normal state

The question of the underlying band particle-hole asymmetry often comes up in these materials at low doping. One way to "factor out" this asymmetry that is extrinsic to the particle-hole mixture measure, is to factor out the normal-state conductances; namely, one can take a ratio of $dI/dV_{\pm}(\mathbf{r}_i,V,T)$ to their proper normal-state values at high temperatures $T>T_c$:

$$dI/dV_{\pm}(\mathbf{r}_i,E,T) \to \frac{dI/dV_{\pm}(\mathbf{r}_i,E,T)}{dI/dV_{\pm}(\mathbf{r}_i,E,T>T_c)}. \tag{14}$$

This procedure will factor out the particle-hole asymmetry for the underlying band and will allow more direct measure of particle-hole asymmetry.

B. Lattice model of a *d*-wave superconductor with broken translation symmetry

One of the most interesting aspects of the response of superconductors to defects is that the defects can probe the properties of the superconducting state that may result in local breaking of the Cooper pairs.[13] The simplest example of such pair breaking defects is magnetic impurities in singlet superconductors, where magnetic scattering disrupts pairing in the singlet channel. Pair breaking defects are known to lead to the formation of bound quasiparticle states in conventional nodeless superconductors.[14] These states are localized in the neighborhood of the defects and can have a very anisotropic structure, depending on the form of the energy gap.[13,15] States, localized near impurities, can carry spin and are expected to modify the ground-state properties of the superconductors as well.

Below we are going to consider a simplified model Eq. (2) with impurities characterized only by the local scalar potential $V^s_{\mathrm{imp}}(i)$. The interplay between all three types of the impurities and their influence on the Bogoliubov angle spatial distribution is an interesting topic by itself, and we are going to consider it in a separate study. We also report on the case of uniform hopping parameter $t_{i,j}\equiv t$.

The superconducting gap function $\Delta\equiv\Delta(\mathbf{r}_i,\mathbf{r}_j)$, where $\mathbf{r}_i$ and $\mathbf{r}_j$ are vectors corresponding to the sites i and j. By making a transformation to variables $\mathbf{R}=(\mathbf{r}_i+\mathbf{r}_j)/2$ and $\mathbf{r}_{ij}=(\mathbf{r}_i-\mathbf{r}_j)/2$, one can notice that the "center of mass" coordinate $\mathbf{R}$ is a "slow" variable, which can be treated as independent from the "fast" variable $\mathbf{r}_{ij}$.

Making the Fourier transform with respect to the fast variable $\mathbf{r}_{ij}$, $\Delta(\mathbf{R},\mathbf{k})=\Sigma_{\mathbf{r}_{ij}}\Delta(\mathbf{R},\mathbf{r}_{ij})\exp(-i2\mathbf{k}\mathbf{r}_{ij})$, one can establish the relationship between the order parameter and the gap function. As is usually done for cuprates, we assume a strong repulsive on-site interaction and a nearest-neighbor attraction. This model is known to produce the *d*-wave pairing signature in the continuum limit $\Delta(\mathbf{R},\mathbf{k})=2\Delta(\mathbf{R})[\cos(ak_x)-\cos(ak_y)]$, where a is the lattice spacing, for the electron densities close to one electron per lattice site. It has been widely and successfully used to describe strong impurities in a *d*-wave superconductor, see Ref. 13. In the real space the *d*-pairing signature is $\eta(\mathbf{r})=\Sigma_{\delta=\pm x,\pm y}(-1)^{\delta}_{\mathbf{r},\mathbf{r}+\delta}$.

In translational invariant case (no impurities) the model gives the $\mathbf{R}$-independent solution,

$$u_{\mathbf{k}} = 1/2[1+\epsilon_{\mathbf{k}}/\Delta(\mathbf{k})],$$

$$v_{\mathbf{k}} = 1/2[1-\epsilon_{\mathbf{k}}/\Delta(\mathbf{k})], \tag{15}$$

where the single-particle energy is given with respect to the chemical potential in the normal state: $\epsilon_{\mathbf{k}}=-1/2t[\cos(k_xa)+\cos(k_ya)]-\mu$. In a general case of the presence of impurities, inhomogeneity, and vortices—which destroy the translational invariance—the solutions are $\mathbf{R},\mathbf{r}$ dependent. Moreover to make progress we would need a numerical solution. We will solve Bogoliubov–de Gennes equations in the real-space representation and $u_{\mathbf{k}},v_{\mathbf{k}}$ amplitudes become an eigenfunctions with eigenvalue index replacing $\mathbf{k}$, see Sec. V.

We will numerically solve the model described by the Hamiltonian Eq. (2) in Sec. V. We will investigate the spatial distribution of BA as a function of position and energy in the case of randomly generated scalar impurity potential V^s_{imp}. The detailed analysis of the effects of other impurities is left for a later presentation. We believe narrowing our analysis down to one kind of impurity would be sufficient to address the spatial inhomogeneity in BA.

III. IMAGING BOGOLIUBOV ANGLE IN NORMAL AND PSEUDOGAP STATES

The BA, as defined, is not sensitive to the superconducting (sc) quantum phase fluctuations. Indeed BA is defined as a function of ratio of the $|u_E(\mathbf{r}_i)|^2/|v_E(\mathbf{r}_i)|^2$. Therefore $\Theta(\mathbf{r}_i,E)$ can be defined even in the presence of such phase fluctuations.[16] Thus, we propose that the discussion about BA be extended to the normal state.

Imagine we are approaching a normal state of superconductor by warming it up. We can see that there will be temperature dependence of the BA. There is no reason to expect an abrupt termination of SC correlations as one crosses T_c. Remnant superconducting correlations are present above T_c,[17,18] and hence one can still have excitations that will have a particle-hole admixture. The difference will be that we are no longer in the state with well defined superconducting Josephson phase.

To illustrate this point, let us consider Bogoliubov-Valatin transformation in the presence of phase fluctuations;

$$\gamma_{n,\uparrow} = u_n(\mathbf{r}_i)c_{n,\uparrow} + \exp[i\phi(\mathbf{r}_i)]v_n(\mathbf{r}_i)c^{\dagger}_{n^*,\downarrow}. \tag{16}$$

Here n and n^* refer to time-reversal partners that form a pair, according to Anderson. We then can use the same definition for BA, Eq. (6) in this case even in the presence of random Josephson phase ϕ. Since one uses amplitudes of u,v, spatial phase disorder does not enter into $\Theta(\mathbf{r}_i,E)$. So for the frozen and presumably for the slowly varying in time phase fluctuations, one can use the BA as defined and image the local particle-hole admixture in the normal state.

One would need to take care of thermal broadening of the tunneling characteristics at higher temperatures. Namely one could divide the tunneling characteristics by derivatives of the Fermi thermal distribution function;

$$\Theta_{\mathrm{PG}}(\mathbf{r}_i,V) = \arctan\left\{\left[\frac{dI/dV_{+}(\mathbf{r}_i,V)f'(E+|eV|)}{dI/dV_{-}(\mathbf{r}_i,V)f'(E-|eV|)}\right]^{1/2}\right\}. \tag{17}$$

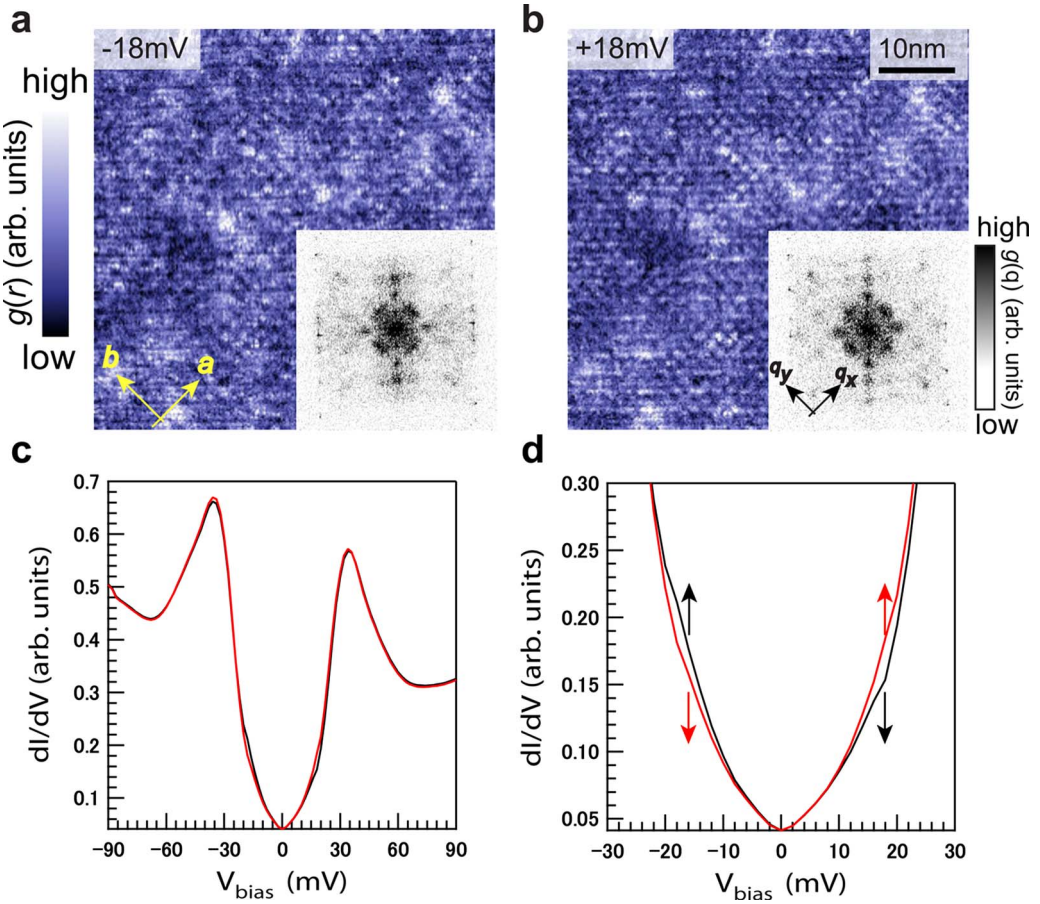

FIG. 3. (Color online) $g(\vec{r},V)$ with 54-nm FOV at (a) $V=-18$ mV and (b) $V=+18$ mV with their Fourier transforms in the insets. The modulations are visible and consist of several wave vectors. (c) Typical averaged spectra taken at different area. (d) Same spectra as (c) but zoomed at the low-energy feature below the maximum gap. Systematic deviation in spectra between the negative and the positive sample biases is seen, as indicated by arrows.

The problem of dynamic phase fluctuations in the state with superconducting fluctuations is complicated. A more detailed analysis would require a specific model for the dynamics of the superconducting phase. An approach to phase fluctuations in PG state using localized Cooper pair states with no long-range phase coherence was advocated in Ref. 19 using STM data.[10]

One can also study the behavior BA for other states, such as flux phase[20] state and density-wave states.[21] Let us consider density-wave states, e.g., *d*-density-wave state (DDW). DDW is often mentioned as a possible state that can explain PG.[21] In any density-wave state, including DDW, particle-hole symmetry is violated and the poles of single-particle excitations are not appearing in pairs symmetrically around chemical potential. Therefore single electron tunneling DOS does not have the components that appear symmetrically at positive and negative biases. If there is a particle-hole symmetric spectrum for DDW state, it can occur only as a special case at one doping level.

Absence of particle-hole symmetry will be easily detected by BA as it will tend to pure hole or particle angle, $\Theta \rightarrow 0,\ \pi/2$. Thus we think BA can be used as a spectroscopy tool to detect presence/absence of superconducting correlations in normal state. Another interesting question to address is how BA behaves upon rising temperature. At low energy it will be close to $\pi/2$ but then it can quickly move away to indicate purely particle or hole states at $T>T_c$ for nonpairing PG state.

These questions go beyond the scope of this paper and will be addressed in a separate publication.

IV. EXPERIMENT

In order to visualize the BA, we have performed an experimental investigation of the spectroscopic imaging scanning tunneling microscopy (SI-STM) measurement on high-temperature superconductor $Bi_2Sr_2CaCu_2O_{8+\delta}$.[22] A single crystal of Bi-2212 grown by floating zone method is hole doped by introducing nonstoichiometric oxygen atoms per unit cell and its hole concentration is adjusted for slightly overdoping ($T_c=89$ K). The crystal is cleaved in the ultrahigh vacuum and immediately inserted into the STM head at $T=4.2$ K. To show the BA, we acquired LDOS images by measuring the STM tip sample differential tunneling conductance $g(\vec{r},V)\equiv dI/dV|_{r,V}$ at each location $\vec{r}$ and bias voltage V. Since LDOS $(\vec{r},E=eV)\propto g(\vec{r},V)$, energy and position dependences of the LDOS are obtained.

In Fig. 3(a), we show a 54-nm $g(\vec{r},V)$ map at

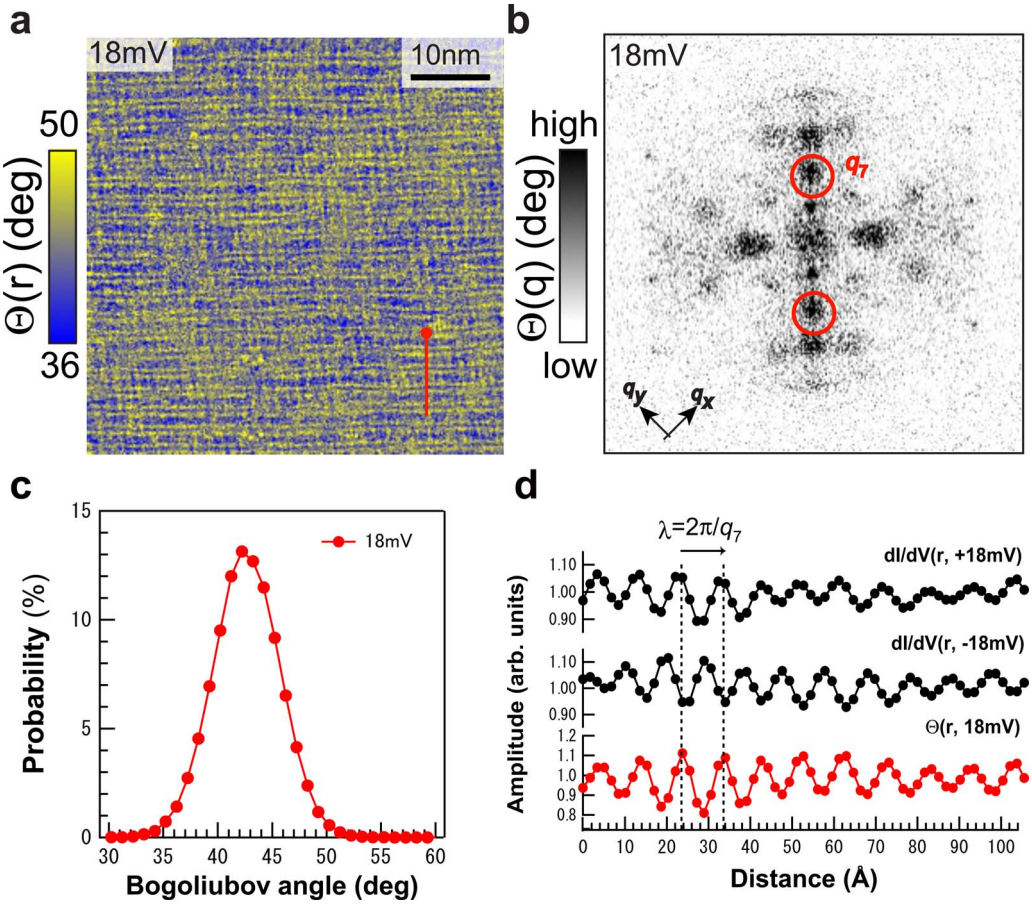

FIG. 4. (Color online) (a) $\Theta(\mathbf{r}_i, V)$ with 54-nm FOV at $V=18$ mV. (b) Fourier transform of $\Theta(\mathbf{r}_i, V)$ in (a). (c) Distribution of $\Theta(\mathbf{r}_i, V)$ at $V=18$ mV. (d) Spatial evolution of the Fourier filtered dI/dV at 18 and −18 mV (black, darker) and $\Theta(\mathbf{r}_i, V=18$ mV) (red, lighter) with $2\pi/q_7$ modulation along the red (light solid) line starting from the solid (red) circle in (a).

$V=-16$ mV measured on the Bi-2212 surface, showing the spatial modulations—which are interpreted as an interference of the Bogoliubov quasiparticles.[23] A Fourier transform of $g(\vec{r}, -18$ mV) in the inset of Fig. 3 exhibits several Fourier spots corresponding to the period of modulation in real space. These observations are consistent with previous reports.[24,25] Although similar modulations are visible in $g(\vec{r}, +18$ mV) shown in Fig. 3, which is the same field of view (FOV) as Fig. 3(a), one can notice that the spatial phase of these modulations is different. dI/dV spectra, which are averaged over the regions with the same gap size, where $g(\vec{r}, -18$ mV) in Fig. 3(a) is slightly higher/lower than the average value, see black/red curves in Fig. 3(c). Overall feature of the spectra taken with different intensity of $g(\vec{r}, -18$ mV) with the same gap are almost identical. However, the significant differences at low energies in the spectra are seen in the Fig. 3(d). It is obvious that the spectrum with relatively higher amplitude at the negative sample bias has the relatively smaller amplitude at the positive sample bias (and vice versa). This implies that the particle and the hole in the superconducting state are entangled with each other.

In Fig. 4(a), we calculate a local BA $\Theta(\mathbf{r}_i, V)$ by taking the ratio of the positive and the negative sample biases $g(\vec{r}, V)$, using the following simple formulas:

$$Z(\mathbf{r}_i, V) \equiv \frac{\frac{dI}{dV}(\mathbf{r}_i, +V)}{\frac{dI}{dV}(\mathbf{r}_i, -V)}, \tag{18}$$

$$\Theta(\mathbf{r}_i, V) = \arctan(\sqrt{Z}). \tag{19}$$

Taking the ratio has an advantage of canceling out the unknown matrix element involved in dI/dV.[26] Fig. 4(a) is the BA map at $V=18$ mV with its Fourier transform, and we found that the $\Theta(\mathbf{r}_i, 18$ mV) shows spatial modulations as well as dI/dV map in Fig. 3 but with more stronger contrast. As seen in Fig. 3(d), the amplitude of dI/dV between positive and negative biases is anticorrelated so that taking the ratio enhances such structure, namely, spatial modulations. BA map is essentially different from the dI/dV map since BA map exhibits the degree of spatial particle-hole mixture of the Bogoliubov quasiparticles. However, as evidenced by the Fourier transform of $\Theta(\mathbf{r}_i, 18$ mV) [Fig. 4(b)], the Fourier pattern is qualitatively the same as those of Figs. 3(a) and 3(b)—indicating that the period of the existing modulation in the BA map is similar to dI/dV modulations. This similarity supports the claim that the local particle and hole

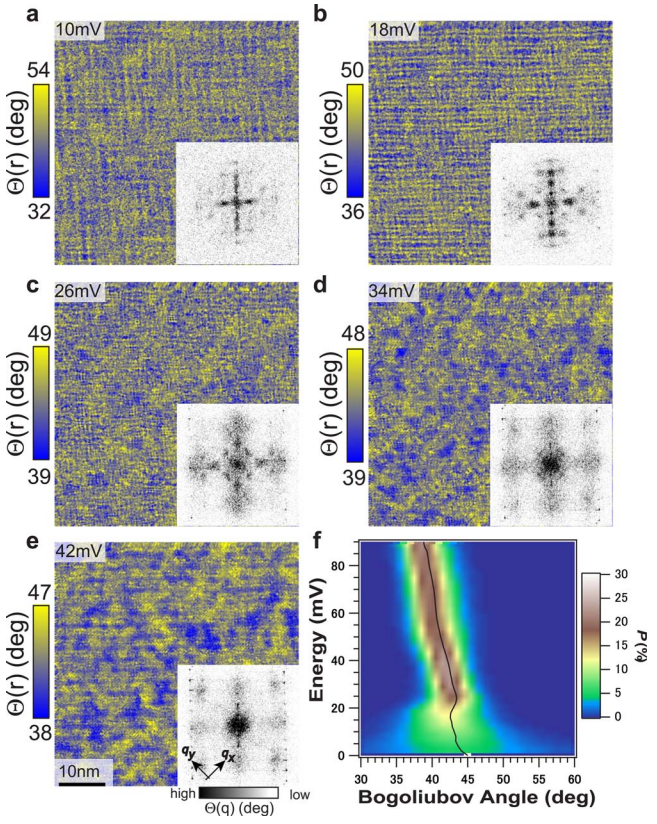

FIG. 5. (Color online) (a)–(e) Images of the BA at each bias voltages ($V=10$, 18, 26, 34, and 42 mV) and their Fourier transforms. (f) Distributions of the BA at each bias voltages from 0 to 90 mV. Peak positions of the histogram are traced by black line.

amplitudes are modulated by scattering. Taking the ratio of dI/dV in Eq. (18) and taking the BA map in Eq. (19) can therefore be important tools to search for the true spatial modulations and individual Fourier spots in the electron density of states.

In Fig. 4(c), we show the distribution of BA at energy, $V=18$ mV, which is peaked at $\Theta=43$ deg, not exactly at 45 deg. One possibility is that the apparent shift of the distribution is caused by asymmetric background in the tunneling spectrum[27] that is sampled more at higher voltage as we shall see in the Fig. 5(f). To visualize the particlelike and holelike regions more clearly, line cuts of BA at $V=18$ mV as well as dI/dV at $V=+18$ and -18 mV—along the trajectory shown in Fig. 4(a)—are exhibited in Fig. 4(d). For simplicity, we only focus on the specific q vector in Fig. 4(b) so that the line profiles are taken from the Fourier filtered dI/dV and $\Theta(\mathbf{r}_i, V=18$ mV) with q_7 vector highlighted by red circle in Fig. 4(b). Particlelike and holelike regions are spatially modulating along the line and clearly show the antiphase behavior in modulation between dI/dV at +18 and −18 mV.

Figures 5(a)–5(e) show the $\Theta(\mathbf{r}_i, V)$ maps for various bias voltages and their Fourier transforms. With increasing energy, the periods of modulation in real space change and corresponding Fourier spots in the inset of the Figs. 5(a)–5(e) move, following the octet model.[23] These observations are consistent with previous reports.[24,25] In addition to the period of modulation, one can immediately notice that the pattern of the spatial modulation changes. At low energies [Figs. 5(a) and 5(b)], spatial modulations are visible all over the field of view. On the other hand, at $V=34$ mV (or $V>34$ mV), such modulations tend to be visible in the restricted area. This difference implies that the different type of scattering might kick in at $V=34$ mV (or $V>34$ mV).

In Fig. 5(f), we show the 2D distribution of the BA in which distributions are normalized at each energies. The spatial change in the BA map seems to occur as a crossover, and it can be realized by deviation of the BA from $\Theta=45$ deg in the Fig. 5(f). The energy, which differentiates the spatially coherent excitations and the localized excitations, is estimated to be ~26 mV (less than mean $\Delta\sim40$ mV) where BA starts to monotonically decrease.

The visualization of the BA will help us to understand the quasiparticle excitations in the superconducting state. The interferences of the Bogoliubov quasiparticles can be understood as a spatial variation of relative weight of the particle and the hole amplitudes, which is represented by the BA. The BA can be a measure of the energy scale of the coherent excitations. Moreover, since the spatial modulations in the electronic structure are revealed much more clearly in the BA map, this provides an excellent technique to determine the momentum space (q space) electronic structure using SI-STM. Hanaguri *et al.*[28] recently demonstrated the power of this technique with the discovery of the interference of the Bogoliubov quasiparticles in Na-CCOC.

V. NUMERICAL SIMULATIONS

In this section we implement simple but realistic mean-field model of an optimally doped cuprate superconductor at zero temperature with disorder. In real materials the quantum fluctuations may give rise to spatial inhomogeneity of local characteristics, including the Bogoliubov angle, without the presence of any impurities. On the other hand, the mean-field description cannot capture quantum fluctuations, and without impurities it will give a perfect translationally invariant solution. In order to model fluctuations of local superconducting characteristics without going beyond the mean-field treatment, we assume a disorder in the system.

We use a simple BCS solution to illustrate the approach on how one can visualize the superconducting admixture of particles and holes in the natural Bogoliubov excitations in superconducting state in the case of broken translational invariance due to disorder. Even though the model is simplistic the approach itself is quite general.

Using the Bogoliubov-Valatin transformation to the quasiparticles operators $\gamma_{n\sigma}$ given by Eq. (5) and by the mean-field approximation, one can diagonalize the Hamiltonian Eq. (2). The quasiparticle amplitudes on lattice sites $(u_n(\mathbf{r}_i), v_n(\mathbf{r}_i))$ have to satisfy inhomogeneous Bogoliubov–de Gennes equations;[29]

$$\begin{pmatrix} \hat{\xi} & \hat{\Delta} \\ \hat{\Delta}^* & -\hat{\xi}^* \end{pmatrix} \begin{bmatrix} u_n(\mathbf{r}_i) \\ v_n(\mathbf{r}_i) \end{bmatrix} = E_n \begin{bmatrix} u_n(\mathbf{r}_i) \\ v_n(\mathbf{r}_i) \end{bmatrix}, \tag{20}$$

where the kinetic operator $\hat{\xi}$ and superconducting order parameter $\hat{\Delta}$ can be represented as

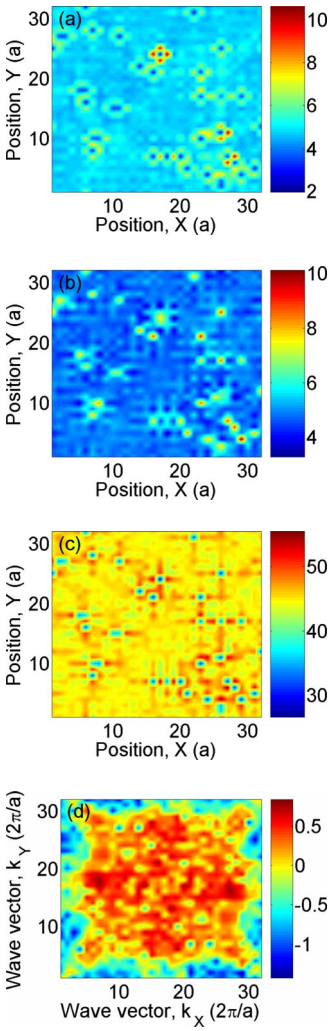

FIG. 6. (Color online) (a)–(d) Calculated LDOS on a square 32×32 lattice at $T=0$. We assume 40 randomly placed impurities with individual impurity strength $V^s_{\rm imp}=1t$. The pairing strength is set to $V_{\rm int}=-2t$ and the chemical potential is set to $\mu=0$ (see text). (a) Calculated local $\frac{dI}{dV}$ tunneling conductance at positive bias $V=0.4t$. (b) Calculated local $\frac{dI}{dV}$ tunneling conductance at negative bias $V=-0.4t$. (c) Corresponding Bogoliubov angle $\Theta(x,y)$. (d) logarithm of the absolute value of Fourier transform of BA $\log_{10}[|\Theta(k_x,k_y)|]$ with subtracted average value $\langle\Theta(x,y)\rangle=45$ deg.

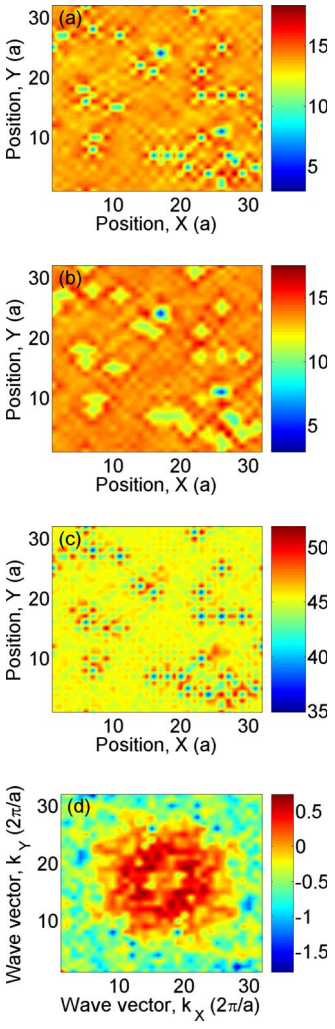

FIG. 7. (Color online) (a)–(d) calculated LDOS on a square 32×32 lattice at $T=0$. We assume 40 randomly placed impurities with individual impurity strength $V^s_{\rm imp}=1t$. The pairing strength is set to $V_{\rm int}=-2t$ and chemical potential is set to $\mu=0$ (see text). (a) Calculated local $\frac{dI}{dV}$ tunneling conductance at positive bias $V=0.8t$. (b) Calculated local $\frac{dI}{dV}$ tunneling conductance at negative bias $V=-0.8t$. (c) Corresponding Bogoliubov angle $\Theta(x,y)$. (d) logarithm of the absolute value of Fourier transform of BA $\log_{10}[|\Theta(k_x,k_y)|]$ with subtracted average value $\langle\Theta(x,y)\rangle=45$ deg.

$$\hat{\xi}u_n(\mathbf{r}_i) = -t\sum_{\boldsymbol{\delta}} u_n(\mathbf{r}_i+\boldsymbol{\delta}) + [V^s_{\rm imp}(\mathbf{r}_i)-\mu]u_n(\mathbf{r}_i),$$

$$\hat{\Delta}v_n(\mathbf{r}_i) = \sum_{\boldsymbol{\delta}} \hat{\Delta}_{\boldsymbol{\delta}}(\mathbf{r}_i)v_n(\mathbf{r}_i+\boldsymbol{\delta}), \tag{21}$$

where $\boldsymbol{\delta}=\pm\hat{\mathbf{x}},\pm\hat{\mathbf{y}}$ are the nearest-neighbor vectors for a square lattice. In case of translational invariant solutions $\hat{\xi}$ becomes $\epsilon_{\mathbf{k}}$ as defined earlier in Sec. II.

We solve Eq. (20) together with the self-consistency condition;

$$\Delta_{\boldsymbol{\delta}}(\mathbf{r}_i) = \frac{V_{\rm int}}{2}\sum_n [u_n(\mathbf{r}_i+\boldsymbol{\delta})v_n^*(\mathbf{r}_i) + u_n(\mathbf{r}_i)v_n^*(\mathbf{r}_i+\boldsymbol{\delta})]\tanh(E_n/2k_BT), \tag{22}$$

where the summation is over the positive eigenvalues E_n only.

For a square lattice system with $L\times L$ lattice sites, the solution of the Bogoliubov–de Gennes equations Eq. (20) is equivalent to the eigenproblem for a $2L^2\times2L^2$ Hermite matrix. In order to minimize the boundary effects for a finite-size system we assume periodic boundary conditions in both x and y directions.

We have performed numerical simulations on a square lattice 32×32 at $T=0$. We assume 40 impurities randomly

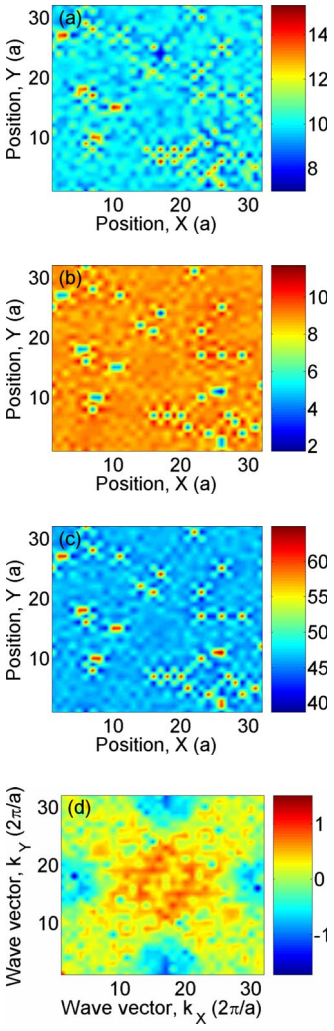

FIG. 8. (Color online) (a)–(d) Calculated LDOS on a square 32×32 lattice at $T=0$. We assume 40 randomly placed impurities with individual impurity strength $V^s_{\text{imp}}=1t$. The pairing strength is set to $V_{\text{int}}=-2t$ and chemical potential is set to $\mu=0$ (see text). (a) Calculated local $\frac{dI}{dV}$ tunneling conductance at positive bias $V=1.2t$. (b) Calculated local $\frac{dI}{dV}$ tunneling conductance at negative bias $V=-1.2t$. (c) Corresponding Bogoliubov angle $\Theta(x,y)$. (d) logarithm of the absolute value of Fourier transform of BA $\log_{10}[|\Theta(k_x,k_y)|]$ with subtracted average value $\langle\Theta(x,y)\rangle=45$ deg. The Fourier transform we obtain is consistent with FT intensity us seen in the experiment, see inset in Fig. 5(e). Please note rotation of (q_x,q_y) basis.

placed on the lattice, each impurity has strength $V^s_{\text{imp}}=1t$. It corresponds to approximately 3% doping. We set $V_{\text{int}}=-2t$ and a half-filled band $\mu=0$.

The results of our numerical simulations are summarized in Figs. 6–8, where we show three panels of plots for calculated local tunneling conductance dI/dV at positive and negative biases using Eq. (9)— the corresponding Bogoliubov angle $\Theta(x,y)$, using Eq. (12)— and the logarithm of the absolute value of its Fourier transform. We consider the following values for the bias: $V=\pm0.4t$, $\pm0.8t$, $\pm1.2t$. Note that at bias $V=\pm0.4t$, which is under the gap value $\Delta\approx0.8t$, the pattern of the local Bogoliubov angle [see Fig. 6(c)] is rotated 45 degrees with respect to the patterns calculated at higher biases $V=\pm0.8t$ [near the gap, see Fig. 7(c)]

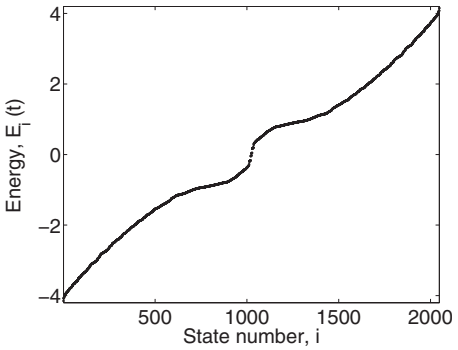

FIG. 9. Calculated 2048 eigenvalues for a 32×32 inhomogeneous two-dimensional system with 40 randomly laced impurities. Note that the symmetry of the numerically obtained eigenvalues with respect to zero and the closed gap for the *d*-wave pairing symmetry.

and $V=\pm1.2t$ [above the gap, see Fig. 8(c)]. The sites on the lattice where there is a large particlelike component of the Bogoliubov excitation, the hole component is small. Complementary pattern is observed on opposite bias. This "rotation" is commonly present in the whole field of view.

In addition, in Fig. 9 we plot the calculated eigenvalues for the random impurity distributions, shown in Figs. 6–8. Obtained eigenvalues just slightly go beyond the energy interval $[-4t,4t]$, which is reproduced for the translational invariant case. This is what one would expect for moderate impurity strength.

To characterize the effect of the local impurities on the local density of state, we plot in Fig. 10 the LDOS at two sites as a function of energy (applied local bias). One site is chosen to be far from impurity $(x,y)=(2,2)$ and another is chosen at the impurity site $(x,y)=(6,6)$. Note that LDOS at the impurity site has relatively lower peaks at energy values of the order of the gap energy $E=\pm0.8t$.

We also present BA along the diagonal line cut for our numerical calculation to compare with experimental results. We observe an out-of-phase angle change for low-energy vs

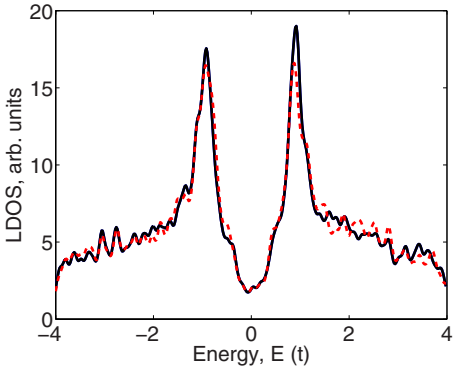

FIG. 10. (Color online) Local density of states as a function of energy at the position (2,2) (solid black line) and at the local impurity site, at the position (6,6) (dashed red line). The difference in LDOS on impurity vs away from impurity results in spatial variations in BA is shown in Figs. 6–8 for different bias values $V=\pm0.4t$, $\pm0.8t$, $\pm1.2t$. The positive bias values are depicted using arrows.

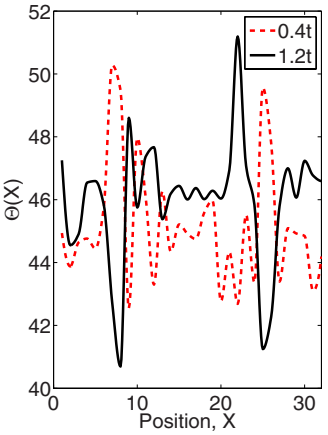

FIG. 11. (Color online) Profile of the Bogoliubov angle Θ along the line cut for bias values $0.4t$ as the red (dashed) line and $1.2t$ as the black (solid) line. The line cut is taken along the direction [1,1]. Note the angle inversion effect with respect to the optimal mixing angle value of 45 deg for low-energy and high-energy BAs.

high-energy BAs, Fig. 11. This out-of-phase behavior is consistent with the behavior seen in Fig. 4.

To further elaborate on the utility of the BA in visualizing particle-hole admixture in paired state, we present here results of numerical solution for the case where we have two competing interactions. One is the superconducting pairing interaction $V_{\rm int}$ and another one is the single-particle potential $V^s_{\rm imp}$. Single-particle potential $V^s_{\rm imp}$ modulation is lined up and forms stripelike patterns, as can be seen in Figs. 12 and 13. For the case when pairing interaction is larger then the single-particle potential $V_{\rm int}=2V^s_{\rm imp}=2t$ we find that Bogoliubov angle is essentially 45 deg across the whole field of view, Fig. 12. In the opposite case when $V^s_{\rm imp}=2V_{\rm int}=2t$ we see substantial variations of the BA across the sample with large departures from optimal value of 45 deg, see Fig. 13.

We thus observe that BA as a concept could be useful in differentiating between states with dominant pairing interactions vs gapped state due to nonsuperconducting order, such as CDW and SDW.

VI. CONCLUSION

In conclusion, we have introduced a spectroscopic measure, Bogoliubov angle $\Theta(\mathbf{r}_i,E)$. This measure allows one to

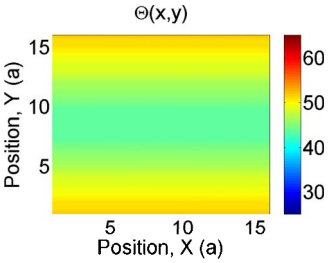

FIG. 12. (Color online) Profile of the Bogoliubov angle Θ for the stripelike pattern of single impurity sites. In this case $V_{\rm int}=2V^s_{\rm imp}$, and we see in the whole field of view predominantly 45 deg angle reflecting strong superconducting correlations.

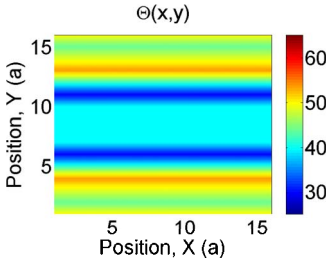

FIG. 13. (Color online) Same as above. In this case $V^s_{\rm imp}=2V_{\rm int}$, and we see substantial modulations of the BA.

image local particle-hole admixture in the superconducting state and in the normal state with superconducting correlations.

The Bogoliubov angle can be studied as a function of position. It can also contain nontrivial Fourier components. This could allow us to make connection with the spatial interference of quasiparticles in superconducting state.[23,28,30,31] Complementary to the momentum space information, one can look at the energy dependence of BA. Energy dependence observed experimentally clearly indicates that there is a change in behavior in $\Theta(\mathbf{r},E)$ at $E\simeq 20-25$ meV, Figs. 4 and 5. This energy range clearly correlates with the changes in the interference patterns. We interpret these changes as an evidence for a change in the superconducting coherence that is weakened at higher energies.

As a future application, we propose that BA be studied as a function of doping and temperature. One can use this to investigate BA and particle-hole at temperatures above T_c for studies of the nature of the pseudogap phase. Using Bogoliubov angle, one could identify how robust the particle-hole mixture is in the normal state and therefore be able to differentiate between different scenarios of PG state.

ACKNOWLEDGMENTS

We are grateful to I. Martin, A. Yazdani, N. Nagaosa, M. Randeria, O. Fischer, W. S. Lee, and Z. X. Shen for the enlightening discussions. This work was supported by the BES and LDRD funds from U.S. Dept. of Energy at Los Alamos National Laboratory under Contract No. DE-AC52-06NA25396. J.C.D acknowledges support from Brookhaven National Laboratory under Contract No. DE-AC02-98CH1886 with the U.S. Department of Energy, from the U.S. Department of Energy Award No. DE-FG02-06ER46306, and from the U.S. Office of Naval Research.

APPENDIX A: ANDERSON MAPPING

Here we recall the Anderson[12] mapping of reduced BCS model on the effective spin model. The reduced BCS Hamiltonian is taken to be

$$H_{\rm red}=-\sum_{\mathbf{k}}(\epsilon_{\mathbf{k}}-\mu)(1-n_{\mathbf{k}}-n_{-\mathbf{k}})-\sum_{\mathbf{k}\neq\mathbf{k}'}V_{\mathbf{k},\mathbf{k}'}c^{\dagger}_{\mathbf{k}}c^{\dagger}_{-\mathbf{k}}c_{-\mathbf{k}'}c_{\mathbf{k}'}$$
$$=-2\sum_{\mathbf{k}}(\epsilon_{\mathbf{k}}-\mu)s_{z,\mathbf{k}}-1/2\sum_{\mathbf{k},\mathbf{k}'}(s^{+}_{\mathbf{k}}s^{-}_{\mathbf{k}'}+s^{+}_{\mathbf{k}'}s^{-}\mathbf{k}),\qquad\text{(A1)}$$

where we assumed translational invariance for simplicity and omit spin indices. Spin operators are defined as

$$s_{z,\mathbf{k}} = 1 - n_{\mathbf{k}} - n_{\mathbf{k}'}, \tag{A2}$$

$$s_{\mathbf{k}}^{+} = b_{\mathbf{k}}^{+} = c_{\mathbf{k}}^{\dagger} c_{-\mathbf{k}}^{\dagger}, \tag{A3}$$

$$s_{\mathbf{k}}^{-} = b_{\mathbf{k}} = c_{\mathbf{k}} c_{-\mathbf{k}}, \tag{A4}$$

and they represent a complete spin algebra over space $n_{\mathbf{k}} - n_{-\mathbf{k}} = 0$, the so-called hard-core boson constraint. z component of the spin corresponds to state with well defined particle number and $s^{\pm}$ corresponds to pairing correlations. Anderson showed that this reduced Hamiltonian describes the spin $s_{\mathbf{k}}$ in an "external" field pointing at an angle $\Theta_{\mathbf{k}}$,

$$\Theta_{\mathbf{k}} = 1/2 \frac{\sum_{\mathbf{k}'} V_{\mathbf{k}\mathbf{k}'} \sin \Theta_{\mathbf{k}}}{\epsilon_{\mathbf{k}} - \mu}. \tag{A5}$$

One immediately recognizes this as a self-consistency equation for BCS solution once we assume $V_{\mathbf{k}\mathbf{k}'}$ to be constant in a range near Fermi surface. Excitation spectrum for the effective spin model is

$$E_{\mathbf{k}} = \left[(\epsilon_{\mathbf{k}} - \mu)^2 + 1/4 \left(\sum_{\mathbf{k}'} V_{\mathbf{k}\mathbf{k}'} \sin \Theta_{\mathbf{k}'} \right) 2 \right]^{1/2}. \tag{A6}$$

Complete identification with Bogoliubov quasiparticles is clear if one identifies

$$\sin \Theta_{\mathbf{k}} = 2 u_{\mathbf{k}} v_{\mathbf{k}}, \quad \cos \Theta_{\mathbf{k}} = u_{\mathbf{k}}^2 - v_{\mathbf{k}}^2. \tag{A7}$$

To make a contact with BA, we notice that in the case of broken translational symmetry we can work out exactly the same representation based on eigenfunctions in real space $u_n(\mathbf{r}_i)$, $v_n(\mathbf{r}_i)$. Then, the mapping on the spin problem will be done in real space; angle $\Theta_{\mathbf{k}}$ is proportional to the BA defined in the Introduction, and we will have $\Theta_E(\mathbf{r}_i)$ as defined in Eq. (6). One can immediately see the direct connection with the Anderson angle used in this effective spin model.

APPENDIX B: NUMERICAL DETAILS

The numerical solution of Eq. (20) together with the self-consistency condition Eq. (22) requires iterative solution and it is organized as follows: (1) For a reasonable initial value of the order parameter $\Delta_{\boldsymbol{\delta}}(\mathbf{r}_i)$ we solve the eigenproblem Eq. (21) to obtain the quasiparticle amplitudes $[u_n(\mathbf{r}_i), v_n(\mathbf{r}_i)]$ and the quasiparticle spectrum E_n. (2) Then, substituting $[u_n(\mathbf{r}_i), v_n(\mathbf{r}_i)]$ and E_n into Eq. (22), we compute an approximation of the order parameter $\Delta_{\boldsymbol{\delta}}^{(\mathrm{appr})}(\mathbf{r}_i)$. (3) In order to avoid numerical instabilities during iterations, we use a mixing scheme $\Delta_{\boldsymbol{\delta}}^{(n+1)}(\mathbf{r}_i) = \alpha \Delta_{\boldsymbol{\delta}}^{(\mathrm{appr})}(\mathbf{r}_i) + (1-\alpha)\Delta_{\boldsymbol{\delta}}^{(n)}(\mathbf{r}_i)$, where $\Delta_{\boldsymbol{\delta}}^{(n)}(\mathbf{r}_i)$ is the order parameter at the previous iteration step. Adjustable parameter α is a number between zero and one. To ensure convergence, we increase the current value of α by 5% if the relative deviation between two consequent steps $S^n = \max_{i,\boldsymbol{\delta}} |\Delta_{\boldsymbol{\delta}}^n(\mathbf{r}_i) - \Delta_{\boldsymbol{\delta}}^{n-1}(\mathbf{r}_i)| / \max_{i,\boldsymbol{\delta}} |\Delta_{\boldsymbol{\delta}}^n(\mathbf{r}_i)|$ has decreased—S^n case, $S^n > S^{n-1}$. (4) The computed $\Delta_{\boldsymbol{\delta}}^{(n+1)}(\mathbf{r}_i)$ is used for the next iteration step.

We repeat iterations until we achieve the acceptable level of accuracy ($\epsilon = 10^{-3}$). After the end of the procedure, we perform an additional step with $\alpha = 1$ to ensure convergence of the obtained solution. It usually takes 20–40 iterations to converge.

[1] M. F. Crommie, C. P. Lutz, and D. M. Eigler, Nature (London) **363**, 524 (1993).
[2] E. J. Heller, M. F. Crommie, C. P. Lutz, and D. M. Eigler, Nature (London) **369**, 464 (1994).
[3] H. C. Manoharan, C. P. Lutz, and D. M. Eigler, Nature (London) **403**, 512 (2000).
[4] J. R. Schrieffer, *Theory of Superconductivity* (Addison-Wesley, Redwood City, 1983).
[5] M. Ma and P. A. Lee, Phys. Rev. B **32**, 5658 (1985).
[6] A. Yazdani, B. A. Jones, C. P. Lutz, M. F. Crommie, and D. M. Eigler, Science **275**, 1767 (1997).
[7] I. Martin and A. V. Balatsky, Physica C **125**, 341 (2000).
[8] E. W. Hudson, K. M. Lang, V. Madhavan, S. H. Pan, H. Eisaki, S. Uchida, and J. C. Davis, Nature (London) **411**, 920 (2001).
[9] M. E. Flatte and D. E. Reynolds, Phys. Rev. B **61**, 14810 (2000).
[10] Michael Vershinin, Shashank Misra, S. Ono, Y. Abe, Yoichi Ando, and Ali Yazdani, Science **303**, 1995 (2004).
[11] Øystein Fischer, Martin Kugler, Ivan Maggio-Aprile, Christophe Berthod, and Christoph Renner, Rev. Mod. Phys. **79**, 353 (2007).
[12] P. W. Anderson, Phys. Rev. **112**, 1900 (1958).
[13] A. V. Balatsky, I. Vekter, and J. X. Zhu, Rev. Mod. Phys. **78**, 373 (2006); A. V. Balatsky, M. I. Salkola, and A. Rosengren, Phys. Rev. B **51**, 15547 (1995); M. I. Salkola, A. V. Balatsky, and J. R. Schrieffer, *ibid.* **55**, 12648 (1997).
[14] L. Yu, Acta Phys. Sin. **21**, 75 (1965).
[15] M. I. Salkola, A. V. Balatsky, and D. J. Scalapino, Phys. Rev. Lett. **77**, 1841 (1996).
[16] V. J. Emery and S. A. Kivelson, Nature (London) **374**, 434 (1995).
[17] J. Corson, R. Mallozzi, J. Orenstein, J. N. Eckstein, and I. Bozovic, Nature (London) **398**, 221 (1999).
[18] Z. A. Xu, N. P. Ong, Y. Wang, T. Kakeshita, and S. Uchida, Nature (London) **406**, 486 (2000).
[19] Han-Dong Chen, Oskar Vafek, Ali Yazdani, and Shou-Cheng Zhang, Phys. Rev. Lett. **93**, 187002 (2004); Z. Tesanovic, *ibid.* **93**, 217004 (2004).
[20] Patrick A. Lee, Naoto Nagaosa, and Xiao-Gang Wen, Rev. Mod. Phys. **78**, 17 (2006).
[21] S. Chakravarty, R. B. Laughlin, D. K. Morr, and C. Nayak, Phys. Rev. B **63**, 094503 (2001).
[22] S. H. Pan, J. P. O'Neal, R. L. Badzey, C. Chamon, H. Ding, E. J. R. Engelbrecht, Z. Wang, H. Eisaki, S. Uchida, A. K. Gupta, K. W. Ng, E. W. Hudson, K. M. Lang, and J. C. Davis, Nature (London) **413**, 282 (2001).
[23] Q. H. Wang and D. H. Lee, Phys. Rev. B **67**, 020511(R) (2003).

[24] K. McElroy, R. W. Simmonds, J. E. Hoffman, D.-H. Lee, J. Orenstein, H. Eisaki, S. Uchida, and J. C. Davis, Nature (London) **422**, 592 (2003).
[25] J. E. Hoffman, K. McElroy, D.-H. Lee, K. M. Lang, H. Eisaki, S. Uchida, and J. C. Davis, Science **297**, 1148 (2002).
[26] Y. Kohsaka, C. Tailor, K. Fujita, A. Schmidt, C. Lupien, T. Hanaguri, M. Azuma, M. Takano, H. Eisaki, H. Takagi, S. Uchida, and J. C. Davis, Science **315**, 1380 (2007).
[27] W. Rantner and X.-G. Wen, Phys. Rev. Lett. **85**, 3692 (2000).
[28] T. Hanaguri, Y. Kohsaka, J. C. Davis, C. Lupien, I. Yamada, M. Azuma, M. Takano, K. Ohishi, and H. Takagi, Nat. Phys. **3**, 865 (2007).
[29] M. Franz, C. Kallin, and A. J. Berlinsky, Phys. Rev. B **54**, R6897 (1996); M. Franz, C. Kallin, A. J. Berlinsky, and M. I. Salkola, *ibid.* **56**, 7882 (1997).
[30] L. Capriotti, D. J. Scalapino, and R. D. Sedgewick, Phys. Rev. B **68**, 014508 (2003).
[31] L. Zhu, W. A. Atkinson, and P. J. Hirschfeld, Phys. Rev. B **69**, 060503(R) (2004).